Exchange Interactions between Two Nitronyl Nitroxide or Iminyl Nitroxide Radicals Attached to Thiophene and 2,2'-Bithienyl Rings

ARTICLE *in* JOURNAL OF THE AMERICAN CHEMICAL SOCIETY · MARCH 1995

Impact Factor: 12.11 · DOI: 10.1021/ja00114a010

4 AUTHORS, INCLUDING:

Katsuya Inoue
Hiroshima University
1,242 PUBLICATIONS **25,317** CITATIONS

SEE PROFILE

Hiizu Iwamura
Nihon University
376 PUBLICATIONS **7,954** CITATIONS

SEE PROFILE

Exchange Interactions between Two Nitronyl Nitroxide or Iminyl Nitroxide Radicals Attached to Thiophene and 2,2′-Bithienyl Rings

Teruyuki Mitsumori, Katsuya Inoue, Noboru Koga, and Hiizu Iwamura*

Contribution from the Department of Chemistry, Graduate School of Science, The University of Tokyo, 7-3-1 Hongo, Bunkyo-ku, Tokyo 113, Japan

Received September 16, 1994[⊗]

Abstract: Eight bis(nitronyl nitroxide) and bis(iminyl nitroxide) diradicals having thiophene (**2,4NT**, **2,5NT**, **2,4IT**, and **2,5IT**) and 2,2′-bithienyl units (**4,4′NB**, **3,3′NB**, **4,5′IB**, and **5,5′IB**) as couplers were prepared. Both **2,5NT** and **4,4′NB** crystallized in monoclinic space group $P2_1/n$ with a = 12.430(2) Å, b = 13.968(4) Å, c = 12.470(2) Å, β = 107.26(1)°, and Z = 4 and with a = 10.766(7) Å, b = 10.186(3) Å, c = 11.625(4) Å, β = 1199(3)°, and Z = 2. The dihedral angles between the imidazoline and thiophene rings were only 6 and 10° in **2,5NT** and 21° in **4,4′NB**. The 2,2′-bithienyl chromophore assumed a planar *anti*-conformation. A dimer structure with the oxygen atom in one molecule and the nearest nitrogen atom in the other at a distance of 3.9 Å stacks linearly along the b axis in **2,5NT**. Each nitronyl nitroxide group at both ends of the **4,4′NB** molecule is in close contact with that of the neighboring molecule to make a one-dimensional chain. EPR spectra of all the diradicals in frozen toluene solutions showed typical fine structures due to triplet states with hyperfine splitting with nitrogen as well as the signals due to $\Delta m_S = 2$ transitions. The zero-field splitting constants were determined as $|D/hc|$ = 0.0071, 0.0085, 0.0066, 0.0108, and 0.0149 cm^{-1} for **2,4NT**, **2,5NT**, **2,4IT**, **2,5IT**, and **3,3′NB**, respectively. Temperature dependence of the EPR triplet signal intensities in the monothiophene derivatives suggested that the triplets would be ground states in the 2,4-isomers and that they are excited states lying above singlet ground states by ΔE_{ST} (= $2J$) = −218 k_B and −52 k_B K in **2,5NT** and **2,5IT**, respectively. The couplings for **2,4NT** and **2,4IT** were determined to be J_{intra}/k_B = 40 and 16 K ($H = -2J_{intra}S_1S_2$ for an S-T model), respectively, by SQUID measurements. Similar data were analyzed in terms of a linear four-spin model ($H = -2J_{intra}(S_1S_2 + S_3S_4) - 2J_{inter}S_2S_3$) for **2,5NT** and an S-T model for **2,5IT** to give J_{intra}/k_B = −114.6, J_{inter}/k_B = −34, and θ/S (S + 1) = −0.8 K and J_{intra}/k_B = −29.7 and $\theta/S(S + 1)$ = −2.5 K, respectively. In the four bithienyl derivatives, the interaction was weak with $|J_{intra}/k_B|$ values being less than 10 K. The signs were barely judged to be positive for **4,5′IB** and negative for **3,3′NB** and **5,5′IB**. Manganese(II) bis(hexafluoroacetylacetonate) formed a microcrystalline complex with **2,4NT** which underwent the transition to a ferrimagnet at 11 K, demonstrating the potentiality of **2,4NT** as a multi(monodentate) triplet diradical coupler.

Introduction

Originally synthesized by Ullman nearly 20 years before,[1] 4,5-dihydro-4,4,5,5-tetramethylimidazole-1-oxyl 3-oxide, alias nitronyl nitroxide (**N**), experienced a wonderful rebirth in the late 1980s as a versatile, persistent organic free radical for exploiting spin ordering in organic molecules and molecular assemblies. In an effort to prepare super-high-spin organic polyradicals by aligning the electron spins within the polymer molecules, poly(phenylacetylene)s carrying **N** on every repeating unit have been prepared.[2] While **N** was kept intact during the Rh-catalyzed polymerization of the monomer phenylacetylenes and the polymer samples having a stoichiometric amount of unpaired electrons were obtained, they were just paramagnetic. The expected ferromagnetic interaction among the radical centers by means of the spin polarization of the intervening π-electrons was not detected. Steric inhibition of the cross-conjugation in the main chain and/or pendant side chains was most probably responsible for the failure to obtain super-high-spin polyradicals. **N** and its 2-alkyl and 2-aryl derivatives serve as bis(monodentate) ligands for coordinatively unsaturated transition metal complexes. They form basically one-dimensional chains, but some of them were found to show macroscopic alignment of spins with the aid of a weak interchain interaction in crystals as represented by the $Mn(hfac)_2$ complex of 2-isopropyl-**N** with a critical temperature of 7.6 K.[3] More recently, the β-form crystals of 2-(*p*-nitrophenyl) derivative (**PNN**) of **N** were found to undergo a transition to the first purely organic ferromagnets at 0.6 K.[4] A number of similar 2-substituted derivatives of **N** have been tested to find better results.[5]

In order to overcome some of the above difficulties and improve the partly successful results, we have come up with the idea of introducing a thiophene ring in place of the benzene ring in the 2-phenyl derivatives of **N** on the following grounds. As the thiophene ring is more electron-rich than the benzene

[⊗] Abstract published in *Advance ACS Abstracts*, February 15, 1995.

(1) Ullman, E. F.; Boocock, D. G. B. *J. Chem. Soc., Chem. Commun.* **1969**, 1161. Ullman, E. F.; Osiecki, J. H.; Boocock, D. G. B.; Darcy, R. *J. Am. Chem. Soc.* **1972**, *94*, 7049.

(2) Fujii, A.; Ishida, T.; Koga, N.; Iwamura, H. *Macromolecules* **1991**, *24*, 1077.

(3) (a) Dickman, M. H.; Porter, L. C.; Doedens, R. *Inorg. Chem.* **1986**, *25*, 2595. (b) Caneschi, A.; Gatteschi, D.; Dessoli, R.; Rey, P. *Acc. Chem. Res.* **1989**, *22*, 392. (c) Caneschi, A.; Ferraro, F.; Gatteschi, D.; Rey, P.; Sessoli, R. *Inorg. Chem.* **1990**, *29*, 4217.

(4) Turek, P.; Nozawa, K.; Shiomi, K.; Awaga, K.; Inabe, T.; Maruyama, Y.; Kinoshita, M. *Chem. Phys. Lett.* **1991**, *180*, 327. Tamaru, M.; Nakazawa, Y.; Shiomi, D.; Nozawa, K.; Hosokoshi, Y.; Ishikawa, M.; Takahashi, M.; Kinoshita, M. *Chem. Phys. Lett.* **1991**, *86*, 401.

(5) Inoue, K.; Iwamura, H. *Chem. Phys. Lett.* **1993**, *207*, 551. Awaga, K.; Inabe, T.; Nakamura, T.; Matsumoto, M.; Maruyama, Y. *Mol. Cryst. Liq. Cryst.* **1993**, *232*, 69. Veciana, J.; Rovira, C.; Hernandez, E.; Molins, E.; Mass, M. *Mol. Cryst. Liq. Cryst.* **1993**, *232*, 163.

0002-7863/95/1517-2467$09.00/0

Chart 1

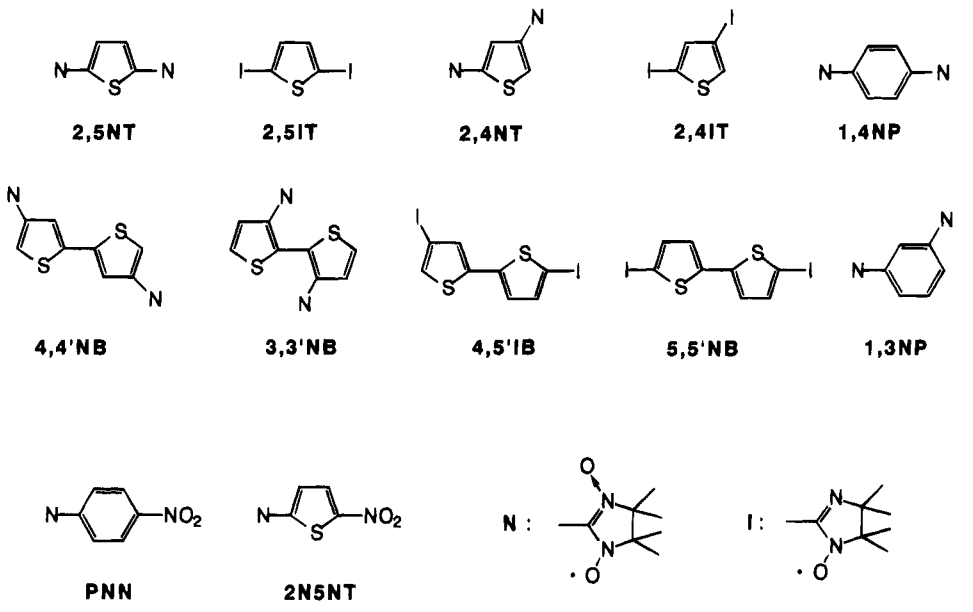

ring, the former is expected to stabilize the electron-attracting nitroxide radicals more strongly. The five-membered rings are sterically less demanding than the six-membered rings to bulky substituents attached to it in keeping co-planarity. While it is electron-rich, the thiophene ring is more stable toward oxidation as demonstrated by the doping of "poly(thiophene)s" for promoting their electric conductivity;[6] the π-conjugation appeared to us to be more robust than the other systems.

Since the new skeletons are not alternant hydrocarbons, the parity rule based on the π-spin polarization mechanism is not straightforwardly applicable to predicting the sign of the exchange coupling between the neighboring radical sites in thiophenes (**T**) and 2,2′-bithienyls (**B**); it is necessary to test the sign and magnitude of the interaction through the thiophene rings. In this paper, we have studied by means of EPR spectroscopy and SQUID susceptometry how two unpaired electrons on two **N** groups or two 4,5-dihydro-4,4,5,5-tetramethylimidazole-1-oxyl (iminyl nitroxide, **I**) groups would interact when attached to thiophene and 2,2′-bithienyl skeletons. The latter would serve as dimer models for poly(thiophene)s carrying those radicals on every repeating unit.

While thiophene is five-membered, it is established to have aromaticity due to the contribution of a pair of π-electrons from the sulfur atom to the aromatic sextet. Therefore, the parity rule established for benzene and biphenyl should be applicable to thiophene and 2,2′-bithienyl, respectively. In the benzenoid series, *m*-phenylene and 3,4′-biphenyldiyl are popular ferromagnetic coupling units in that the electron spins of the two radical centers attached to them align in parallel.[7] Studies of the electronic structures of the diradicals attached to aromatic five-membered rings are not without precedents. 3,4-Furandiyl, pyrroledilyl, and thiophenediyl units have been studied extensively by Berson and co-workers, and their singlet ground states are discussed in terms of the heteroatom-perturbed tetramethyleneethanes.[8] 2,5-Disubstituted topology has been studied by Lahti and Ichimura.[9] These substitution patterns on the non-alternant heteroaromatic coupling spacers correspond to the *o*- and *p*-phenylene couplers. To our knowledge, there is no precedent for the 2,4-thiophenediyl unit which appears to correspond to the *m*-phenylene parity and therefore is expected to serve as a ferromagnetic coupler.

Furthermore, the potentiality of **2,4NT** as a multi(monodentate) triplet diradical coupler was tested by making its Mn(II) complex and comparing it with *m*- and *p*-phenylenebis **N**.[10]

Results

Preparations of Thiophene and 2,2′-Bithienyl Derivatives Having Two Nitroxide Radicals and Mn(hfac)$_2$·2,4NT. Thiophene and 2,2′-bithienyl derivatives were prepared by a sequence of reactions summarized in Scheme 1. Dibromides[11] were lithiated with *n*- or *tert*-butyllithium and then reacted with *N*,*N*-dimethylformamide to give the diformyl derivatives in high yield. Symmetrical dibromo-2,2′-bithienyls were prepared by coupling of the dibromothiophenes after monolithiation and reaction with $CuCl_2$. In the case of 4,5′-diformyl-2,2′-bithienyl, 4-bromo-2,2′-bithienyl was lithiated directly. According to a general method reported previously,[1] the diformyl derivatives were allowed to react with 2,3-bis(hydroxyamino)-2,3-dimethylbutane. The resulting bis(hydroxyamines) were oxidized with lead oxide to afford a mixture of the substituted nitronyl nitroxide (**N**) and iminyl nitroxide (**I**) diradicals. In the 4,5′- and 5,5′-isomers of the 2,2′-bithienyl derivatives, the **N** moieties were spontaneously reduced to give only **I** radicals as isolable products under similar conditions.[12] The crude nitroxides were separated and purified by chromatography on silica gel. The fortuitously formed radicals **I** were eluted first with *n*-hexane/CH_2Cl_2 and then the radicals **N** were eluted with neat CH_2Cl_2.

(6) Skotheim, T. A., Ed. *Handbook of Conducting Polymers*; Marcel Dekker: New York, 1986.

(7) Itoh, K. *Pure Appl. Chem.* **1978**, *50*, 1251. Iwamura, H. *Pure Appl. Chem.* **1993**, *65*, 57. Iwamura, H. *Mol. Cryst. Liq. Cryst.* **1993**, *232*, 233.

(8) Stone, K. J.; Greenberg, M. M.; Blackstock, S. C.; Berson, J. A. *J. Am. Chem. Soc.* **1989**, *111*, 3659. Greenberg, M. M.; Blackstock, S. C.; Stone, K. J.; Berson, J. A. *J. Am. Chem. Soc.* **1989**, *111*, 3671. Busch, L. C.; Heath, R. B.; Berson, J. A. *J. Am. Chem. Soc.* **1993**, *115*, 9830.

(9) Lahti, P. M.; Ichimura, A. S. *J. Org. Chem.* **1991**, *56*, 3030. Ling, C.; Lahti, P. M. *J. Am. Chem. Soc.* **1994**, *116*, 8784.

(10) Caneschi, A.; Gatteschi, D.; Renard, J. P.; Rey, P.; Sessoli, R. *Inorg. Chem.* **1993**, *32*, 1445.

(11) (a) Ruggli, P. *Ber. Dtsch. Chem. Ges.* **1917**, *50*, 883. (b) Heller, G. *Ber. Dtsch. Chem. Ges.* **1917**, *50*, 1202. (c) Steinkopf, W.; Köhler, W. *Liebigs Ann. Chem.* **1937**, *532*, 250. (d) Ruggli, P. *Helv. Chim. Acta* **1938**, *18*, 845. (e) Hünig, S.; Steinmetzer, H.-C. *Liebigs Ann. Chem.* **1976**, 1090. (f) Nakayama, J.; Fujimori, T. *Sulfur Lett.* **1990**, *11*, 29. (g) Rutherford, D. R.; Stille, J. K.; Elliot, C. M.; Reichert, v. R. *Macromolecules* **1992**, *25*, 2294.

(12) Ullmann, E. F.; Call, L.; Osiecki, J. H. *J. Org. Chem.* **1970**, *35*, 3623. Shimomura, O.; Abe, K.; Hirota, M. *J. Chem. Soc., Perkin Trans. 2* **1988**, 795.

Scheme 1[a]

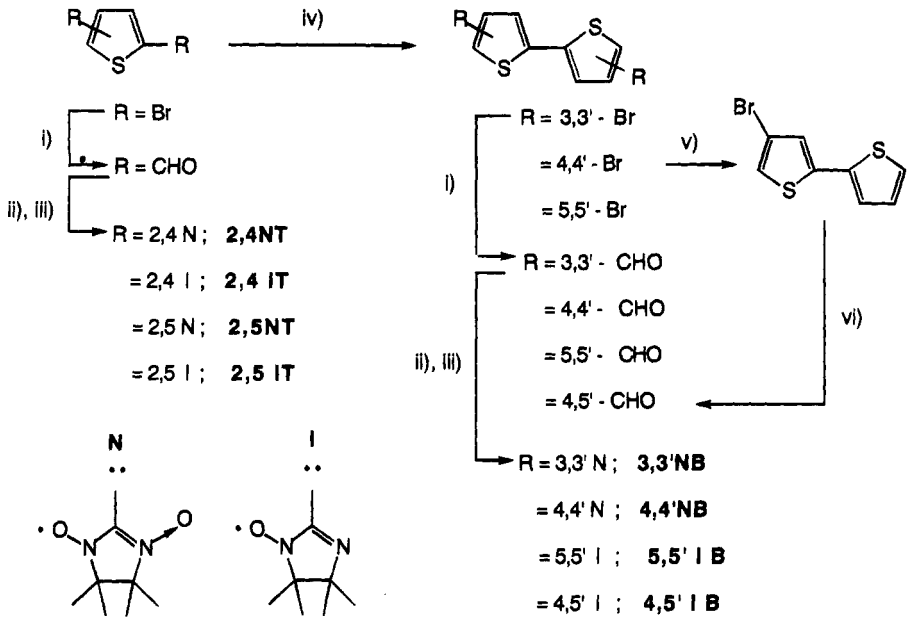

[a] (i) *n*-BuLi, DMF/Et_2O; (ii) (2,3-bis(hydroxyamino)-2,3-dimethylbutane/C_6H_6;; (iii) PbO_2/CH_2Cl_2; (iv) *n*-BuLi, $CuCl_2/Et_2O$; (v) *n*-BuLi, H_2O/Et_2O; (vi) *t*-BuLi, DMF/Et_2O.

Table 1. Crystallographic Data for **2,5NT** and **4,4'NB**

	2,5NT	**4,4'NB**
empirical formula	$C_{18}H_{26}N_4O_4S$	$C_{22}H_{28}N_4O_4S_2$
formula weight	394.49	476.61
cryst color, habit	black, block	black, block
cryst dimens (mm)	0.40 × 0.40 × 0.65	0.75 × 0.50 × 0.50
cryst system	monoclinic	monoclinic
lattice parameters		
a (Å)	12.430(2)	10.766(7)
b (Å)	13.968(4)	10.186(3)
c (Å)	12.470(2)	11.625(4)
β (deg)	107.26(1)	109.88(3)
V (Å^3)	2067.6(8)	1199(2)
space group	$P2_1/n$	$P2_1/n$
Z value	4	2
D_{calc} (g/cm^3)	1.267	1.320
μ (Mo Kα)	B. Int. Measurements	B. Int. Measurements
no. of observations	1727 ($I > 5.00\sigma(I)$)	1062 ($I > 3.00\sigma(I)$)
no. of variables	244	156
residuals: R; R_w	0.068; 0.091	0.073; 0.076

Recrystallization from *n*-hexane gave black crystals of **N** and red to brown crystals of **I**. The samples for X-ray crystallography were obtained by slow evaporation of the solvent from solutions of the diradicals in *n*-hexane.

$Mn(hfac)_2$ complexes of 2,4- and 2,5-bis(1-oxy-3-oxo-4,4,5,5-tetramethyl-2-imidazolinyl)thiophenes (**2,4NT** and **2,5NT**) were prepared by a procedure similar to those employed for the 2-phenyl derivative of **N** in the literature.[3a] Dark green powders of $3Mn(hfac)_2{\cdot}2$(**2,4NT**)$\cdot CH_2Cl_2$ and microcrystals of $Mn(hfac)_2{\cdot}$**2,5NT** were obtained, and their compositions were determined by elemental analyses.

X-ray Crystal Structures of 2,5NT and 4,4'NB. Black block crystals for **2,5NT** and **4,4'NB** were measured on an X-ray diffractometer, and their crystal parameters are listed in Table 1. ORTEP drawings and crystal packings of **2,5NT** and **4,4'NB** are given in Figures 1 and 2, respectively.

In the molecular structure of **2,5NT** (Figure 1a), there is an approximate mirror plane passing through the center of the thiophene ring with which the two **N** rings are nearly coplanar and make dihedral angles of 6 and 10°. One of the oxygen atoms of each **N** unit is only 2.72 Å away from the sulfur atom

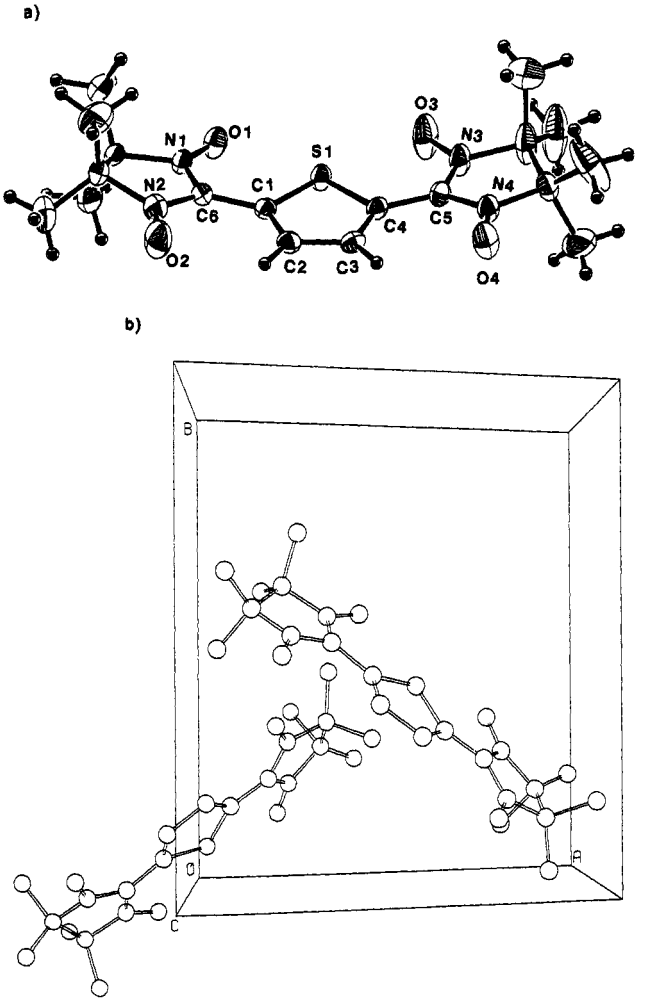

Figure 1. (a) ORTEP drawing of the molecular structure and (b) crystal packing in the unit cell of **2,5NT**.

of the **T** ring. As shown in Figure 1b viewed along the *c* axis, a dimer unit is formed in which both the molecules are nearly orthogonal to each other and the shortest distance is 3.88 Å between the oxygen atom (O4) of one **N** unit and the nitrogen

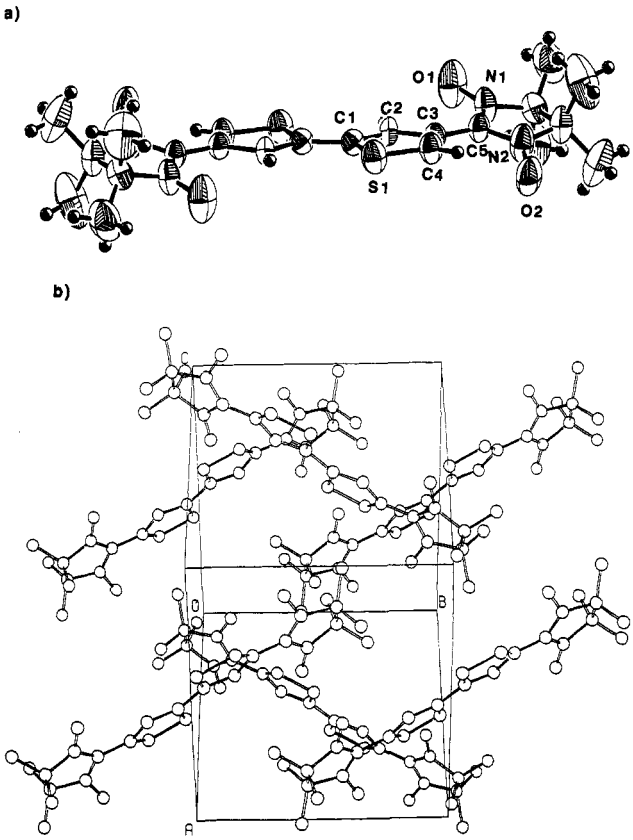

Figure 2. (a) ORTEP drawing of the molecular structure and (b) crystal packing in the unit cell of **4,4′NB**. Only one of the disordered oxygen atoms (O2) is shown.

atom (N1) of the other **N** in the adjacent molecule. The dimer unit stacks linearly along the *b* axis in the crystal.

The 2,2′-bithienyl unit is planar and assumes an *anti*-conformation with respect to the two sulfur atoms in **4,4′NB** (Figure 2a). There is a center of symmetry in the middle of the C2−C2′ bond of the **B** unit which is planar. The dihedral angle of the imidazoline ring plane with the 2,2′-bithienyl skeleton is 21°. In the crystal packing as shown in Figure 2b, each **N** unit of both ends of the **4,4′NB** molecule has another nitronyl nitroxide group of the neighboring molecule in proximity to make a one-dimensional chain. One of the N−O bonds of the **N** unit denoted N2−O2 does not lie in the plane of the imidazoline ring but is disordered in that it is directed either above (+14°) or below (−27°) the mean five-membered ring plane (only the former is shown in Figure 2a). Therefore, the intermolecular distance between the two oxygen atoms along the one-dimensional chain could not be determined uniquely; it was estimated to be 3.95, 3.98, or 4.20 Å. The one-dimensional chains pile crosswise in two parallels, and the nearest distance between the oxygen of **N** on one chain and the sulfur of the **B** unit on the other chain is 3.18 Å.

Since only a tiny monoclinic single crystal was obtained for **2,4IT**, X-ray diffraction was weak and therefore, the number of observations was limited. The refinement of the analysis was also hampered by the presence of the disorder with respect to which nitrogen atom is bonded to the oxygen atom in the **I** unit attached to the 4-position of the thiophene ring. There is no such disorder in the **I** unit at position 2; the oxygen atom is attached to the nitrogen atom near the sulfur atom of the thiophene ring with the intramolecular nonbonding distance between the oxygen and the sulfur atom being ca. 2.90 Å. A crude crystal structure analysis revealed that the imidazoline units are out of the thiophene ring plane by 3 and 16°. The

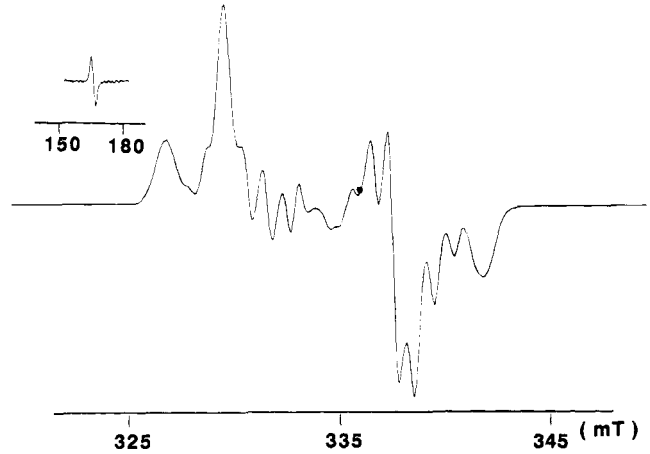

Figure 3. EPR (9.3926 GHz) spectra of **2,4NT** in frozen toluene at 10 K.

flat molecules form a face-to-face dimer in which the distance between the radical centers is 3.4−3.5 Å.

EPR Spectra of Thiophene and 2,2′-Bithienyl Diradicals. EPR spectra of the nitroxide radicals in degassed toluene solutions were measured in the temperature range 10−298 K. At 298 K, **2,4NT** and **2,5NT** showed characteristic five-line spectra (g = 2.0065, a_N = 7.7 G, 2 N)[1] due to hyperfine coupling with two equivalent nitrogen nuclei. **4,4′NB** gave a similar spectrum (g = 2.0067, a_N = 7.8 G). The spectra of **4,5′IB** and **5,5′IB** were of triplet of triplets (g = 2.006, a_N = 13.2 and a_N' = 6.6 G) due to hyperfine coupling with two different nitrogen atoms. Others (**2,4IT**, **2,5IT**, and **3,3′NB**) gave broad singlets.

At 10 K, EPR spectra of all the nitroxide diradicals of the **T** series except **2,5NT** gave fine structures due to dipolar coupling of the unpaired electrons including $\Delta m_S = 2$ transitions at about 160 mT. A typical example of **2,4NT** is given in Figure 3. **2,5NT** showed no significant signals at 10 K but started to give signals due to a triplet species at ca. 40 K. The zero-field splitting (zfs) parameters $|D/hc|$'s were determined from the difference ($2|D/hc|$) between the highest-field (H_z) and lowest-field (H_{-z}) resonances to be 0.0071, 0.0066, 0.0085, and 0.0108 cm^{-1} for **2,4NT**, **2,4IT**, **2,5NT**, and **2,5IT**, respectively. The $|E/hc|$ parameters of them were not obtained as the signals due to the X and/or Y transitions in the $\Delta m_s = 1$ region overlapped heavily by hyperfine coupling with four nitrogen nuclei as observed in Figure 3.

Temperature dependences of the signal intensities due to the triplet states showed sharp contrast between the 2,4- and 2,5-dinitroxide diradicals. As the temperature was elevated from 10 K, the signals due to the triplets of **2,4NT** and **2,4IT** decreased their intensities in accordance with a Curie law. **2,5IT**, on the other hand, showed quite a different behavior; its intensity increased, reached a maximum at 38 K, and then decreased at higher temperatures. The signals due to triplet **2,5NT** appeared at 40 K and continued to increase in intensity with increasing temperature up until 120 K, at which temperature the signals began to broaden, probably due to the softening of the matrix. In order to determine the temperature at which the signal intensity of the triplet species reached a maximum, a poly(vinyl chloride) (PVC) film was employed in place of a frozen toluene solution. The **2,5NT**-doped PVC film was made by slow evaporation of the solvent from a solution of PVC and **2,5NT** (100:3 w/w) in THF. Signals very similar to those obtained in frozen toluene solution grew in at 40 K, reached a maximum at 140 K, and remained up until ca. 300 K (Figure 4). The temperature dependences of the triplet-signal intensities

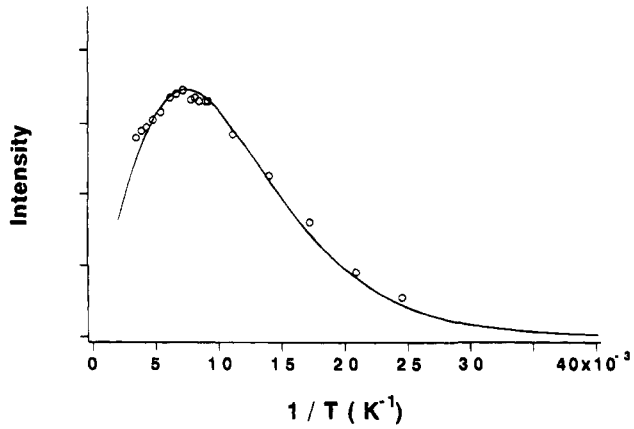

Figure 4. Temperature dependence of the EPR signal intensities of **2,5NT** in PVC films.

(I) strongly suggest that the observed triplet spectra of the 2,4- and 2,5-isomers of **T** are due to ground and thermally populated triplet states, respectively. The energy gaps ($\Delta E_{ST} = 2J$) between the two states were estimated to be -433 and -103 cal/mol (-218 k_B and -52 k_B K) for **2,5NT** and **2,5IT**, respectively, using eq 1 representing the Boltzmann distribution between the two states[13] where C is a proportionality constant.

$$I = \frac{C}{T}\frac{1}{3 + \exp(-2J/k_BT)} \qquad (1)$$

The negative signs in ΔE_{ST} correspond to singlet ground states and antiferromagnetic interactions.

EPR spectra of all the diradicals in the **B** series in toluene glass except for **3,3′NB** showed unseparated fine structures containing shoulders in addition to $\Delta m_S = 2$ transitions at ca. 160 mT, characteristic of triplet species. From their signal width in $\Delta m_S = 1$ transitions, $|D/hc|$ for **4,4′NB**, **4,5′IB**, and **5,5′IB** was estimated to be less than 0.0041, 0.0037, and 0.0042 cm^{-1}, respectively. In the case of **3,3′NB** under similar conditions, triplet fine structures with $|D/hc| = 0.0149$ and $|E/hc| = 0.0002$ cm^{-1} were observed together with the signal at 167 mT. The temperature dependence of the signal intensities due to the triplet states was investigated in the temperature range 10−120 K. In the intensity vs inverse temperature plots (I vs $1/T$), **4,4′NB** and **4,5′IB** gave linear relations in line with the Curie law and **3,3′NB** and **4,4′IB** gave trends which deviated from linearity at the lowest-temperature region. As the deviation did not give a maximum intensity above 10 K, the ΔE_{ST} values were estimated to be $-20 < \Delta E_{ST} < 0$ cal/mol.

Magnetic Susceptibilities of the Diradicals of the Thiophene and 2,2′-Bithienyl Series. Magnetic susceptibilities of the nitroxide diradicals were measured in the temperature range 2−350 K at constant magnetic field of 0.1 or 1 T on a SQUID magnetometer/susceptometer, unless otherwise stated. Microcrystalline or polymer matrix samples of them were employed for the measurements.

The temperature dependences of the molar magnetic susceptibilities (χ_{mol}) of **2,4NT**, **2,5NT**, **2,4IT**, and **2,5IT** are shown in the form of $\chi_{mol}T$ vs T plots in Figure 5. The observed $\chi_{mol}T$ values were 0.73 emu K mol^{-1} or somewhat (~6%) smaller at 350 K, suggesting that the singlet and triplet states are nearly statistically populated at ambient temperature. Their temperature dependences and the analyses in reference to their crystal and molecular structures are given below separately. Similar plots for **3,3′NB**, **4,4′NB**, **4,5′IB**, and **5,5′IB** are shown in Figure 6.

(13) Bleaney, B.; Bowers, K. D. *Proc. R. Soc. London* **1952**, *A214*, 451.

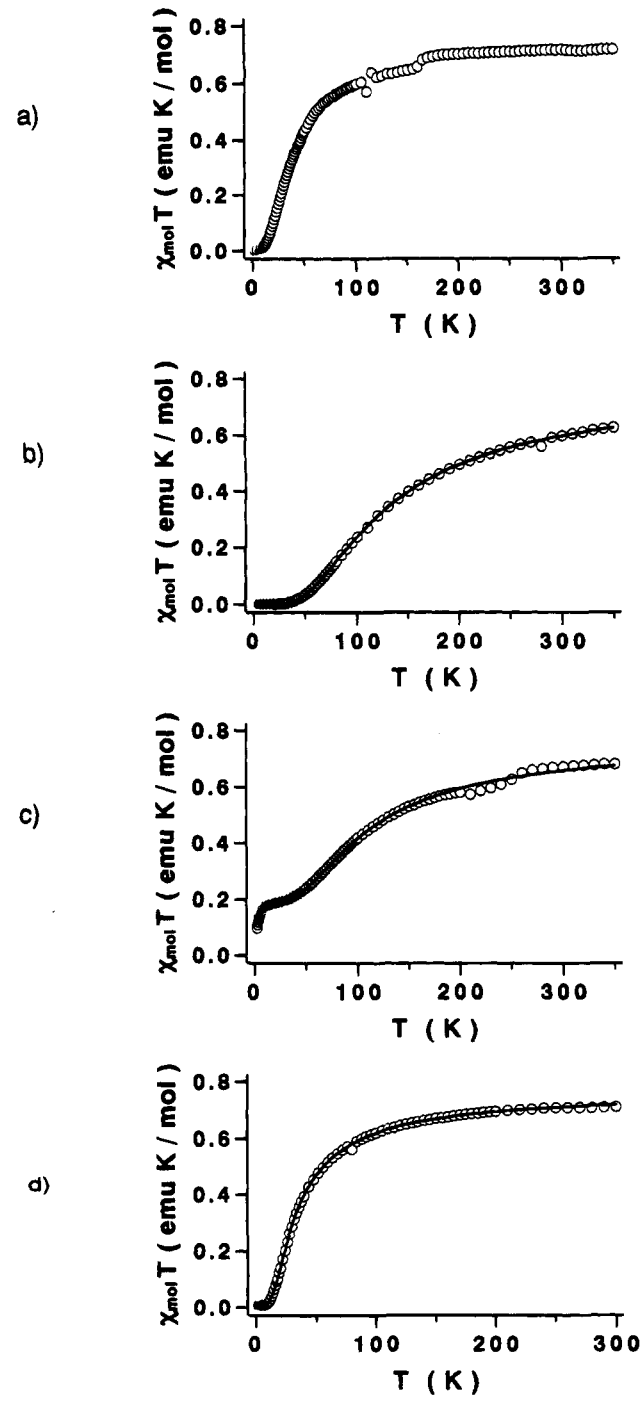

Figure 5. Temperature dependence of the molar magnetic susceptibility (χ_{mol}) as expressed by $\chi_{mol}T$ vs T plots for the diradicals of the thiophene series: (a) **2,4NT**, (b) **2,5NT**, (c) **2,4IT**, and (d) **2,5IT**. The solid curves are theoretical ones as described in the text.

(1) 2,4NT. The $\chi_{mol}T$ values remained almost constant in the temperature range 350−150 K and then decreased sinusoidally to zero as the temperature was lowered. A small discrepancy in the $\chi_{mol}T$ values was observed at 150 and 135 K on sweeping the temperature downward and upward (Figure 5a). This phenomenon was reproducible after the temperature cycle and independent of the samples of **2,4NT**. The presence of a crystal and/or structural phase transition is considered to be responsible, but no further study to confirm this was performed. Although all attempts to fit possible two-spin and linear- and rectangular-four-spin models to the observed $\chi_{mol}T$ vs T plot were unsuccessful, its plot obviously showed strong antiferromagnetic interaction. For exclusion of the intermolecular interaction, **2,4NT** (3.5% w/w) doped in PVC films was

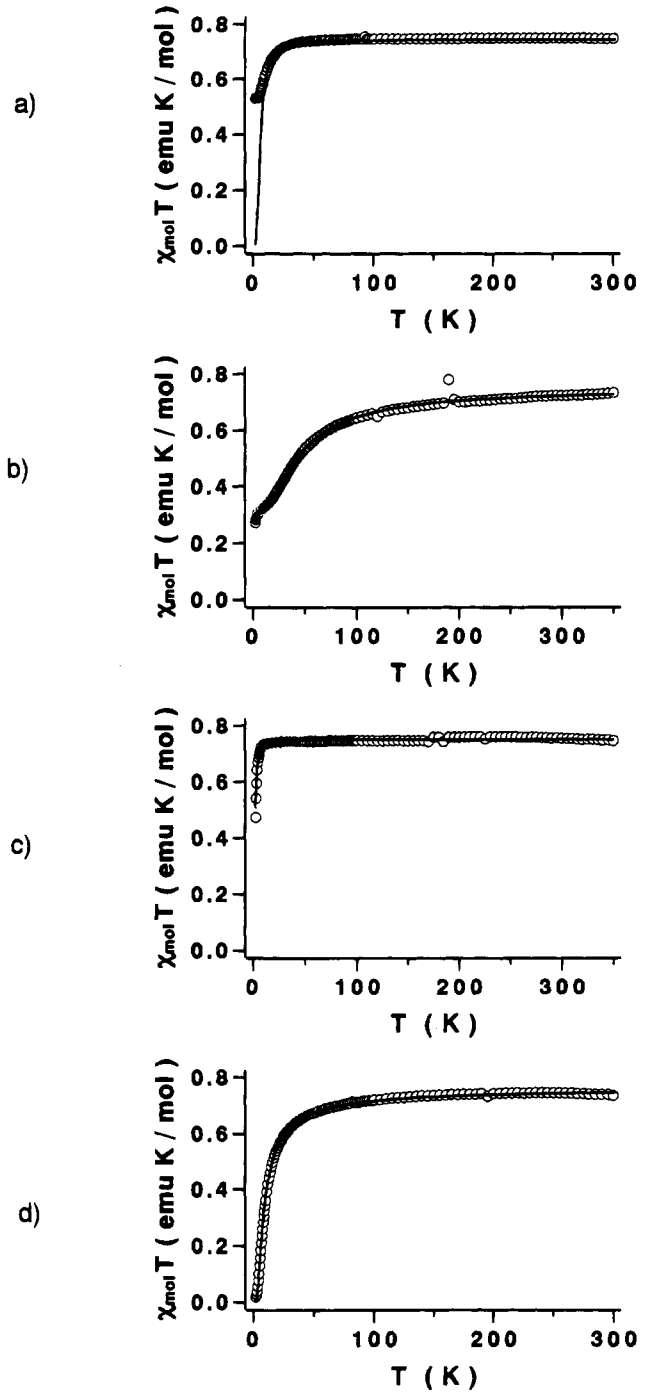

Figure 6. Temperature dependence of the molar magnetic susceptibility (χ_{mol}) as expressed by $\chi_{mol}T$ vs T plots for the diradicals of the 2,2′-bithienyl series: (a) **3,3′NB**, (b) **4,4′NB**, (c) **4,5′IB**, and (d) **5,5′IB**. The solid curves are calculated ones as described in the text.

studied. The $\chi_{mol}T$ vs T plot in the temperature range 2−180 K at a field of 1 T is shown in Figure 7. Most of the antiferromagnetic interaction was excluded. The $\chi_{mol}T$ value was 0.80 emu K mol^{-1} at 1.8 K, increased sharply to 0.88 emu K mol^{-1} at 5.5 K, and then decreased gradually toward 180 K. All the experimental data in this temperature region were obviously higher than 0.73 emu K mol^{-1}, a value for the two spins in the degenerate singlet and triplet state or for the isolated two spins. This temperature dependence of the $\chi_{mol}T$ values was analyzed in terms of a modified singlet−triplet two-state model where the magnetic exchange coupling constant J corresponds to a Hamiltonian of the form $H = -2JS_1S_2$. The Weiss field represented by constant θ was employed to describe the remaining interradical interaction. The g value was fixed

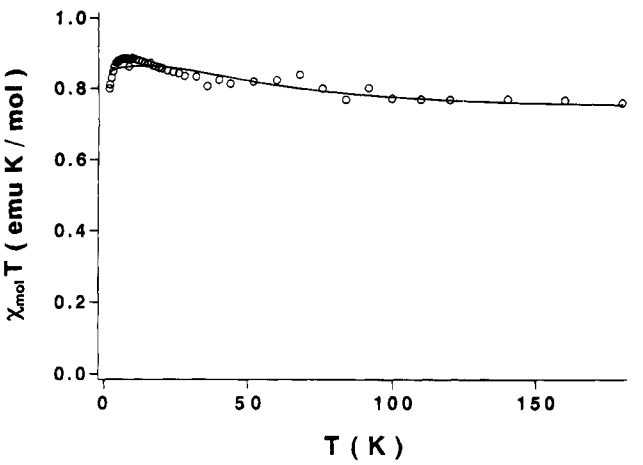

Figure 7. Temperature dependence of the molar magnetic susceptibility (χ_{mol}) as expressed by $\chi_{mol}T$ vs T plots for diradical **2,4NT** diluted in PVC matrix.

$$\chi_{mol} = f\frac{2Ng^2\mu_B{}^2}{k_B(T-\theta)[3+\exp(-2J/k_BT)]} \quad (2)$$

to 2. Purity factor f was introduced for microcrystalline samples of the diradical used for the magnetic measurement.[14] The best-fit parameters by means of a least-squares method were $J = 40 \pm 2$ K, $\theta = -0.04 \pm 0.02$ K, and $f = 0.86$.

(2) 2,5NT. As the temperature was lowered, the $\chi_{mol}T$ values of **2,5NT** decreased continuously to nearly zero as shown in Figure 5b. A linear four-spin model (Scheme 2) was applied

Scheme 2

$$S_1 \overset{J}{\text{——}} S_2 \overset{aJ}{\cdots\cdots} S_3 \overset{J}{\text{——}} S_4$$

to the $\chi_{mol}T$ vs T plot, since the crystal structure of **2,5NT** from the X-ray analysis suggested such an arrangement of the spins in the crystals. The spin Hamiltonian for such a system is given by eq 3 where J and aJ are intra- and intermolecular exchange parameters, respectively. The temperature dependence of the

$$H = -2J(S_1S_2 + S_3S_4) - 2aJ(S_2S_3) \quad (3)$$

magnetic susceptibility χ_{mol} is then given by eq 4 where all symbols have their usual meaning. This equation was fitted to

$$\chi_{mol} = \frac{Ng^2\mu_B{}^2}{6k_BT} \times \frac{30\exp A + 6\exp B + 6\exp D + 6\exp E}{5\exp A + 3\exp B + \exp C + 3\exp D + 3\exp E + \exp F} \quad (4)$$

$$A = -E_Q/k_BT,\ B = -E_{T1}/k_BT,\ C = -E_{S1}/k_BT,\ D = -E_{T2}/k_BT,\ E = -E_{T3}/k_BT,\ F = -E_{S2}/k_BT$$

the experimental data by means of a least-squares method to give the best fit parameters: $J_{intra} = -114.6 \pm 0.4$ K and $J_{inter} = -34 \pm 3$ K. The computed curve is also included in Figure 5b.

(3) 2,4IT. As the temperature was decreased from 350 K, the $\chi_{mol}T$ value of a microcrystalline sample of **2,4IT** started to decrease continuously toward zero, indicating the presence of

(14) Matsumoto, T.; Ishida, T.; Koga, N.; Iwamura, H. *J. Am. Chem. Soc.* **1992**, *114*, 9952.

Scheme 3

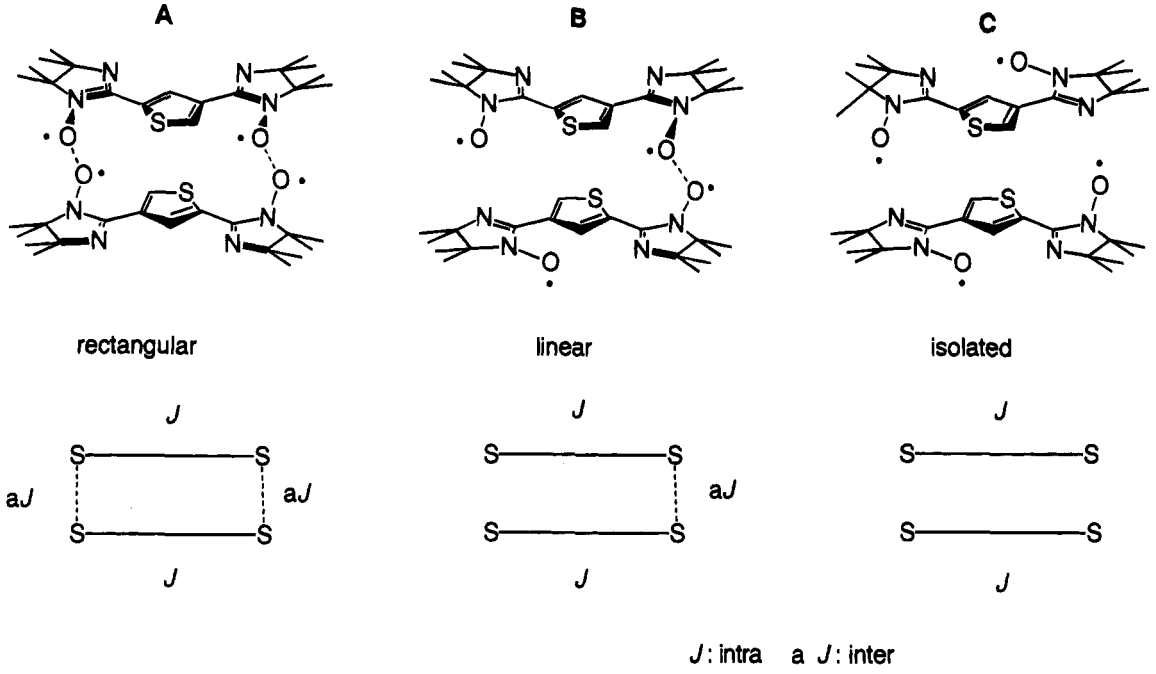

Scheme 4

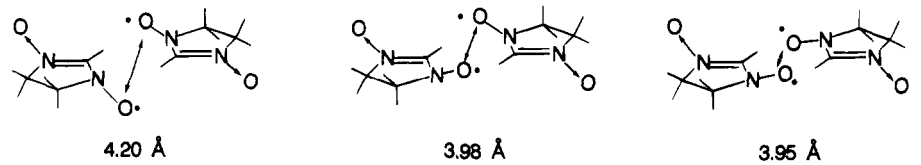

a strong antiferromagnetic interaction in the crystalline sample. The decrease was, however, not monotonous, but there was a small plateau of ca. 0.2 emu K cmol^{-1} at ca. 25 K as shown in Figure 5c. The step-shaped decrease cannot be explained by a simple singlet−triplet model but suggests either the presence of a high-spin state with a considerably large energy gap to the next lower state or a mixture of species having two different negative J values, one large and the other small. As the formation of the face-to-face dimers was suggested by a crude X-ray analysis of **2,4IT**, the strange behavior of the $\chi_{mol}T$ vs T plot in the crystalline state might be caused by interdimer interaction. Taking into account the disorder found for the position of the oxygen atom, we assumed the observed χ_{mol} values consisting of a weighted sum of those due to rectangular-four spin (r) A, linear-four spin (l) B, and magnetically isolated species (i) C (Scheme 3, eq 5).

$$\chi_{mol} = f_r\chi_r + f_l\chi_l + f_i\chi_i \tag{5}$$

A least-squares fitting of the theoretical equation (available as supplementary material) to the observed values of **2,4IT** as represented by the solid curve in Figure 5c gave $J_{intra}/k_B = 16$ K and $J_{inter}/k_B = -105$ K and f values of 63, 25, and 12% for the rectangular, linear four-spin, and isolated two-spin systems, respectively.

(4) 2,5IT. The $\chi_{mol}T$ values of **2,5IT** decreased gradually as the temperature was lowered from 300 to 100 K and more steeply below 100 K (Figure 5d). The temperature dependence was analyzed in terms of a modified singlet−triplet model (eq 6). The best-fit parameters to the observed $\chi_{mol}T$ vs T plot were $J/k_B = -29.7 \pm 0.1$ K and $\theta/S(S+1) = -2.5 \pm 0.2$ K.

(5) 4,4′NB. As the temperature was decreased, the $\chi_{mol}T$ values of **4,4′NB** decreased gradually from 350 to 50 K and in a slightly stepwise manner below 50 K as observed in Figure 6a. The trend could not be reproduced theoretically by a 1D-Heisenberg model, although the result of an X-ray analysis suggested the presence of a linear chain structure. The stair-shaped temperature dependence of the $\chi_{mol}T$ values was also observed in **2,4IT** and might be caused by the disordered position of the oxygen atoms of the **N** unit in the chain structure as indicated in Figure 2. When intramolecular interaction through the **B** unit in **4,4′NB** was ignored and three sorts of direct through-space interaction between the radical centers **N** were assumed as depicted in Scheme 4, the best-fitted parameters were obtained as -0.2 ± 0.3, -36 ± 2, and -74 ± 15 K for J in a ratio of 45 ± 1, 44 ± 1, and 6 ± 1%, respectively, by applying a weighted S-T model.

$$\chi_{mol} = \frac{Ng^2\mu_B{}^2S(S+1)}{3k_B(T-\theta)}$$

$$S(S+1) = \frac{6}{3 + \exp(-2J/k_BT)} \tag{6}$$

$$\theta = CS(S+1)$$

(6) 3,3′NB, 4,5′IB, and 5,5′IB. The $\chi_{mol}T$ vs T plots for **3,3′NB**, **4,5′IB,** and **5,5′IB** were fitted to modified S-T models (eq 6) to give $J/k_B = -6 \pm 0.2$, 3.0 ± 0.2, and -7.5 ± 0.1 K and $\theta/S(S+1) = -2$, -0.9 ± 0.0, and -1.4 ± 0.1 K, respectively. In **3,3′NB**, the experimental data deviated upward from the theoretical curve below 10 K, indicating that a certain ferromagnetic interaction is operative at the low-temperature region.

Magnetization Data for 2,4NT and 4,4′NB. In order to confirm the ground spin states of **2,4NT** and **4,4′NB** more

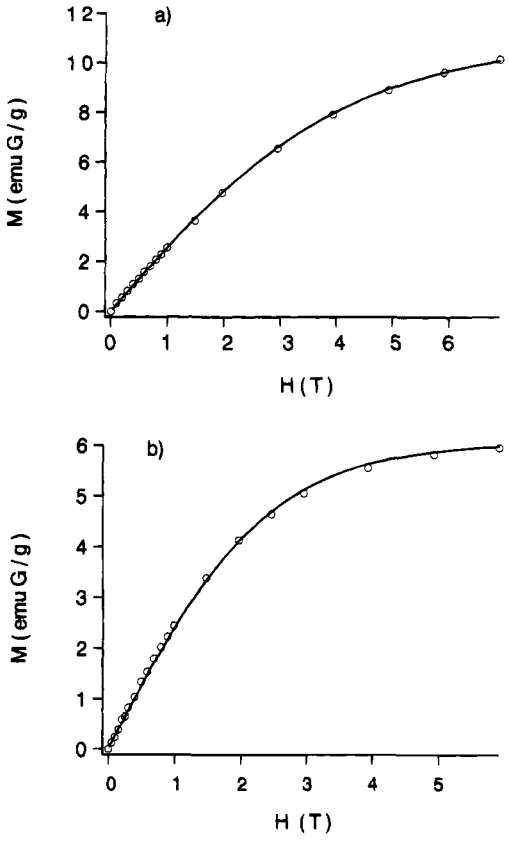

Figure 8. Field dependences of the magnetizations for (a) **2,4NT** at 3.8 K and (b) **4,4NB** at 1.7 K, isolated in toluene solid solutions. Solid curves are drawn according to the theoretical Brillouin functions in which $J = S = 1$ and $^1/_2$, respectively.

precisely, the magnetizations (M) of **2,4NT** and **4,4′NB** isolated in toluene solid solutions (2.7 and 7.2 mM, respectively) were measured at 3.8 and 1.8 K, respectively, on a Faraday magnetic balance as a function of the main field in the range 0−7 T (Figure 8). The experimental data of M obtained for **2,4NT** and **4,4′NB** agreed reasonably well with the theoretical curves represented by the Brillouin function $B_J(x)$ (eq 7) in which $J = S = 1$ and $^1/_2$, respectively.

$$M = NgJ\mu_B B_J(x)$$

$$B_J(x) = \frac{2J+1}{2J}\coth\frac{2J+1}{2J}x - \frac{1}{2J}\coth\frac{1}{2J}x \qquad (7)$$

where

$$x = \frac{gJ\mu_B H}{k_B T}$$

Magnetic Properties of 3Mn(hfac)$_2$·2(2,4NT)·CH_2Cl_2 and Mn(hfac)$_2$·2,5NT Complexes. Dark green powders of 3Mn(hfac)$_2$·2(**2,4NT**)·CH_2Cl_2 and microcrystals of Mn(hfac)$_2$·**2,5NT** were studied by SQUID susceptometry at 1.8−300 K to give the temperature dependence of $\chi_g T$ as reproduced in Figures 9 and 10, respectively.

The $\chi_g T$ value for 3Mn(hfac)$_2$·2(**2,4NT**)·CH_2Cl_2 was 6.85 × 10^{-3} emu K g^{-1} at 300 K at a field of 100 mT. As the temperature was lowered, the $\chi_g T$ values remained constant, began to increase gradually at 140 K and steeply at 12.5 K, and then decreased below 10 K at fields of 100 and 0.5 mT as shown in Figures 9a and 9b, respectively. The magnetization vs temperature curves at a field of 0.5 mT are given in the inset of Figure 9b. The field-cooled magnetization (FCM) measured

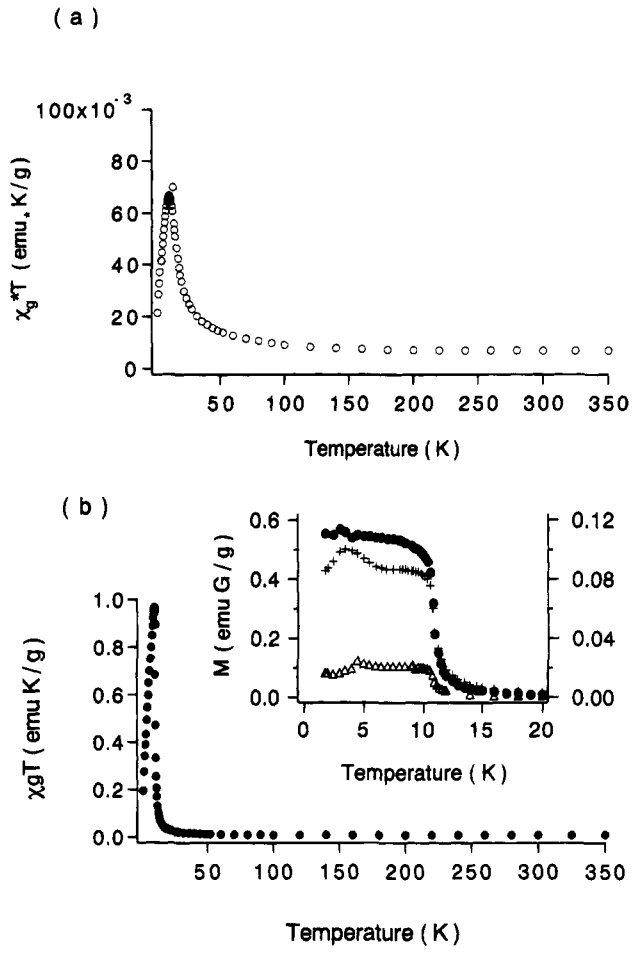

Figure 9. Temperature dependences of χT for the Mn(hfac)$_2$ complex with **2,4NT** in field strengths of (a) 0.5 and (b)100 mT. The Inset of Figure 11b shows the temperature dependence of magnetization at 0.5 mT: field-cooled magnetization (○), zero-field-cooled magnetization (+), and remnant magnetization (△).

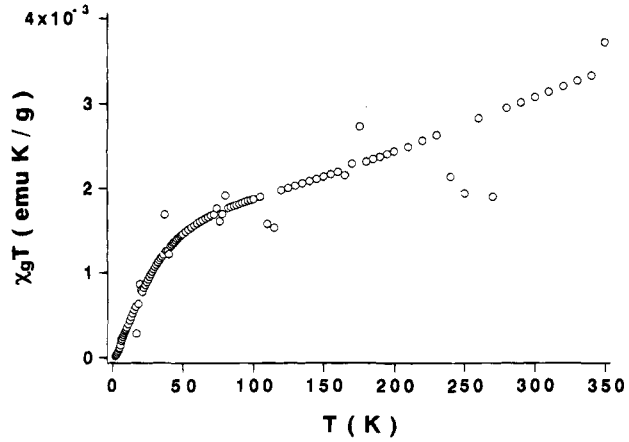

Figure 10. $\chi_g T$ vs T plot for the Mn(hfac)$_2$ complex with **2,5NT**.

upon cooling down within the field showed a rapid increase of M with a change of sign for the second derivative at 11 K. The zero-field-cooled magnetization (ZFCM) measured upon cooling down in zero field and then warming up within the field is also given. When the sample was cooled down in zero field and then warmed up in zero field, a remnant magnetization (REM) was observed, which vanished at 11 K. These data clearly indicate that the sample behaved as a magnet with a spontaneous magnetization below 11 K. When the field dependence of the magnetization was studied in fields of 0−7 T below 11 K, it is noted that the M values increased steeply to ca. 10 emu G g^{-1}

Table 2. Intramolecular Exchange Coupling Parameters for the Diradicals Determined by the Temperature Dependences of the Paramagnetic Susceptibilities (J_M) and EPR Signal Intensities (J_E)

	J_M[a] (K)	J_E[a] (K)
2,5NT	−115	−109
2,5IT	−30	−25
2,4NT	40	>0
2,4IT	16	>0
4,4′NB	≈0	$-10 < J < 0$
3,3′NB	−6	$-10 < J < 0$
4,5′IB	3	>0
5,5′IB	−7.5	$-10 < J < 0$

[a] The magnetic coupling constants quoted correspond to a Hamiltonian of the form $H = -2JS_1S_2$.

Scheme 5[a]

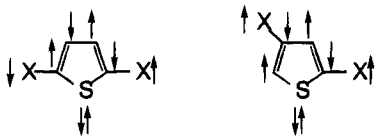

[a] X: radical centers.

in the range 0−30 mT and then gradually from 30 mT and above. At 1.8 K, a hysteresis loop with remnant magnetization of 5.3 emu G g^{-1} and coercive force of 2.2 mT was observed.

On the other hand, complex Mn(hfac)$_2$·**2,5NT** showed an opposite magnetic behavior in the χ_gT vs T plot. The χ_gT value decreased monotonically from 300 K and steeply at cryogenic temperature as shown in Figure 10, suggesting the operation of antiferromagnetic interaction.

Discussion

X-ray Crystal and Molecular Structures. The dihedral angles of the imidazoline rings with the thiophene and 2,2′-bithienyl rings are in the range 6−10° with the exception of such an angle of 21° in **4,4′NB**. All the angles are decidedly smaller than a typical value of 45° in 2-phenyl derivatives of **N**.[4,5,8,10] The observed intramolecular S···O contacts of 2.7−2.9 Å are shorter than the sum of the van der Waals radii (3.32 Å = 1.80 + 1.52 Å) and are considered to be contributing to the co-planarity of the imidazoline rings attached next to the sulfur atom of the thiophene rings. The role of sulfur in controlling the conformation and packing in crystals is well documented.[15] The reduction of the dihedral angles between the imidazoline rings remote from the sulfur atom and the thiophene rings should be ascribed to the diminution in the steric repulsion due to the thiophene ring hydrogens ortho to the substituents; smaller intraring bond angles in the five-membered ring result in the larger extraring angles of the outer hydrogens and the substituents.

Regiospecificity in Intramolecular Exchange Coupling between Two Radical Centers through the Thiophene and 2,2′-Bithienyl Rings. The J values for all eight samples obtained by EPR and SQUID experiments are summarized in Table 2.

The thiophene ring is five-membered and yet maintains aromaticity by incorporating a pair of electrons on the sulfur atom into the aromatic sextet. Therefore, as described in Scheme 5, two radical centers attached to the thiophene ring are expected to interact in the same fashion as in the benzene counterparts; 2,4- and 2,5-diradicals will have intramolecular ferro- and antiferromagnetic interaction, respectively. In other words, a valence bond theoretical picture of the spin polarization via the carbon π-orbitals may be as in alternant hydrocarbons, but a path via the sulfur atom will take advantage of the superexchange of a lone pair of electrons. The predictions based on the two routes are mutually consistent.

Scheme 6

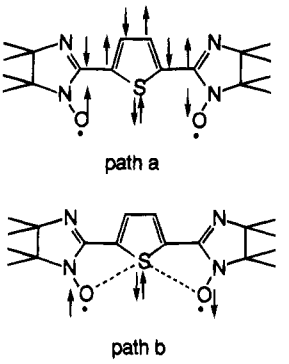

Similarly, the magnetic interactions in 2,2′-bithienyl derivatives are predicted to be similar to those in biphenyl and therefore ferromagnetic in 4,5′-diradicals but antiferromagnetic in 3,3′- and 5,5′-diradicals.[7] 4,4′-Isomers corresponding to biphenyl-*m,m′*-diyl diradicals are vinylogous to tetramethyleneethane, and therefore, singlet and triplet states should be nearly degenerate.[7,16]

(1) Thiophene Diradicals. In the EPR spectra of the 2,4-isomers, both **2,4NT** and **2,4IT** showed signals characteristic of triplet diradicals. The plots of the signal intensity (I) vs inverse temperature followed Curie laws. Ferromagnetic intramolecular interaction for **2,4NT** was corroborated by the magnetization measurement at 3.8 K on a Faraday balance in which the spin quantum number S of unity was found (Figure 8). The J values for the 2,4-isomers were estimated by analyzing the $\chi_{mol}T$ vs T plots in their SQUID susceptibility measurements to be 40 and 16 K for **N** and **I**, respectively. These numbers indicate that the nitronyl nitroxide radicals have stronger interactions than the iminyl nitroxide. Whereas analytically pure (see Experimental Section) parameter f was optimized at 0.86 for **2,4NT**. Any error in the concentration of the unpaired electrons due not only to the sample purity but also to deviation of the g value from 2, weighing the sample, and/or miscalibration of the susceptometer may be accumulated in the f values. The optimization could have been performed without introduction of parameter f, but, since the J values are of interest in this study, f was included in the analysis with the aim of attenuating the dispersion of the fitted J values.

The J/k_B values of ca. −109 and −26 K for the 2,5-isomers of **N** and **I**, respectively, were obtained from the temperature dependences of the EPR signal intensities due to the triplet states and are in reasonable agreement with $J/k_B = -115$ and −26 K obtained by the SQUID susceptibilities. Here again, the interaction is stronger in **N** although negative in sign. The dipolar couplings are, however, greater in **2,5IT** than in **2,5NT**; $|D/hc| = 0.0108$ and 0.0085 cm^{-1}, respectively, indicating that the mean distance between the two unpaired electrons of the former may be smaller than in the latter. Therefore, **2,5IT** is suggested to have a conformation in which both NO bonds are situated near the sulfur atom of the thiophene ring. In this conformation, there are two paths conceivable for the exchange coupling as described in Scheme 6. Paths a and b correspond to through-bond and through-space interaction, respectively, and the latter is aided by a superexchange interaction of a lone pair

(15) Desiraju, G. R. In *Crystal Engineering. The Design of Organic Solids*; Materials Science Monographs; Elsevier: Amsterdam, 1989; Vol. 54, Chapter 7 and references cited therein.

(16) Borden, W. T.; Iwamura, H.; Berson, J. A. *Acc. Chem. Res.* **1994**, *27*, 109.

of electrons on the sulfur atom. Both paths are expected to produce antiferromagnetic interaction. If path b is operative, the J value of **2,5IT** is expected to be larger than that of **2,5NT** since spin density on NO in the **I** unit is larger compared with the one in **N** in which the spin is delocalized on two NO groups. The experimental results do not reflect such a trend. Therefore, path a is considered to be an important path for the magnetic interaction in the 2,5-isomers (Scheme 6).

One of the most important conclusions from this work is that the magnetic interaction between the two nitronyl nitroxide radicals through a thiophene ring is greater in magnitude than those through a benzene ring in the corresponding *m*- and *p*-phenylenebis(nitronyl nitroxide) derivatives **1,3NP** (J/k_B = ca. 0,[10,17c] and 23[17b] K) and **1,4NP** ($J/k_B = -52$ K[10]). The oxygen atom of the nitronyl nitroxide moiety at the α-position of the thiophene ring appears to have strong interaction with the sulfur atom as observed by a short contact of 2.7 Å in Figure 2. Although discredited in the previous paragraph, a further consideration has to be directed to this kind of additional interacting path.

The dihedral angles of the imidazoline ring with the thiophene rings are in the range 6−10° with one exception of 21°. Reported dihedral angles between the two chromophores in the 2-phenyl derivative of **N** range from 32 to 45°.[4,5,8,10,17] The co-planarity and the consequent better spin polarization in the ring in the thiophene derivatives are considered to be the most important factors for the stronger magnetic interaction. The contribution of a 1,3-diene character to the greater interaction through the thiophene rings than through phenylene may not be neglected.[9]

(2) 2,2′-Bithienyl Derivatives. Except for **3,3′NB** for which dipolar coupling constants were determined, the EPR spectra of the other 2,2′-bithienyl diradicals were not well-separated. The plots of the signal intensity (I) vs inverse temperature followed the Curie law, suggesting that $-20 < \Delta E_{ST} < 0$ cal/mol. The conclusions were supported by the magnetic susceptibility measurements; the J/k_B values were all in the range −7.5−0 K. Magnetization measurement of **4,4′NB** in solid toluene on a Faraday balance gave $S = {}^1/_2$ at 1.8 K, indicating that the two nitroxide radicals are either isolated or produce nearly degenerate singlet and triplet states. In spite of the planarity of the molecules, the magnitude of intramolecular interaction between the nitronyl nitroxide units was found to be very weak. Polarization of the π-electron spins on the 2,2′-bithienyl chromophore may not be enough to exchange-couple the two spins on two **N** or **I** units effectively. The singly occupied MO has a node at position 2 of the 4,5-dihydroimidazole-1-oxyl 3-oxide, and therefore, delocalization of the spins to the 2-aryl rings is limited. In order to understand coupling across the center bond of the 2,2′-bithienyl unit more precisely, it could be of help to employ a more delocalizable spin center such as $Ph_2C(\cdot)$-, $PhC(\cdot\cdot)$-, and $-N(\cdot\cdot)$.[14]

Intermolecular Interaction in the Crystals of the Thiophene and 2,2′-Bithienyl Diradicals. Except for **4,5′IB** and **5,5′IB**, all the microcrystalline samples studied by the SQUID susceptometric method showed antiferromagnetic intermolecular interaction. It was most dramatic in 2,4-isomers; while the intramolecular interaction as detected by EPR fine structures for the sample in frozen solution was ferromagnetic, antiferromagnetic interaction was conspicuous in the crystalline state. The strong intermolecular antiferromagnetic interaction overshadowed the intramolecular ferromagnetic interaction. In the case of a sample of **2,4NT** diluted in PVC which prevented the formation of the dimer structure observed in X-ray analysis, a positive J/k_B value of 40 K was actually obtained for the SQUID measurement. Similar strong intermolecular antiferromagnetic interactions were observed in other thiophene derivatives in crystals. It is considered that Coulombic interaction by polarizability for oxygen and nitrogen atoms in nitroxide associated with a sulfur atom plays an important roll for the tight packing of the crystal structure.

Scheme 7

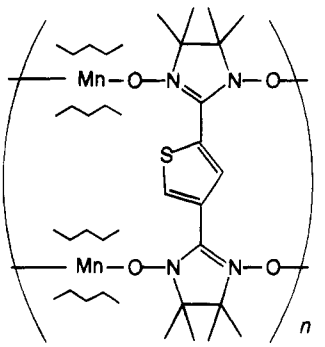

$[2Mn(hfac)_2 \cdot \mathbf{2,4NT}]_n$

Mn(hfac)$_2$·NT's and Their Magnetic Properties. Since the **N** unit can serve as a bis(monodentate) ligand, any **NT** should have four ligating sites at its maximum. In place of a linear chain or a macrocyclic ring made of 2-subsutituted **N** with $Mn(hfac)_2$,[3] formation of a ladder polymer[18] like $[2Mn(hfac)_2 \cdot \mathbf{2,4NT}]_n$ (Scheme 7) or other complexes structured in higher dimension had been expected. The obtained complexes are still deficient in the metal ions.

The $\chi_g T$ value of 6.85×10^{-1} emu K g^{-1} = 15.7 emu K mol^{-1} for $3Mn(hfac)_2 \cdot 2(\mathbf{2,4NT}) \cdot CH_2Cl_2$ at 300 K fits in the order of magnitude with a paramagnetic sample of $S = {}^4/_2$, a theoretical value ($^5/_2$−$^1/_2$) for the occurrence of the antiferromagnetic short-range coupling between the Mn ion and the nitroxide radical in this complex. The strong antiferromagnetic coupling ($J/k_B < -150$ K)[19] explains the lack of a minimum in the $\chi_g T$ vs T plot (Figure 10a) in the temperature range studied. While the transition to a magnet was confirmed to take place at 11 K, the observed magnetization curve which consisted of the extremely field-sensitive and slowly saturating parts suggested that not all but ca. 30% of the unpaired electrons in this powder sample take part in the spontaneous alignment below the critical temperature. The rest of the spins appear to be independent or form less ordered segments. This is not unreasonable as the radical sites are not fully ligated with the manganese ions.

Lack of its transition in $Mn(hfac)_2$·**2,5NT** under similar conditions seems to indicate that intramolecular ferromagnetic interaction in the diradical through the π-conjugated magnetic coupler should be important. Although information on the crystal structures for both complexes could not be obtained, the potentiality of **2,4NT** as a multidentate triplet diradical coupler was amply demonstrated.

Conclusion

Two nitronyl nitroxide radicals separated by the 2,4- and 2,5-thiophenediyl units interact ferro- and antiferromagnetically with $\Delta E_{ST} = 2J/k_B = 80$ and −229 (−218 by EPR) K, respectively.

(17) (a) Dulog, A.; Kim, J. S. *Angew. Chem., Int. Ed. Engl.* **1990**, *29*, 415. (b) Izuoka, A.; Fukuda, M.; Sugawara, T. *Mol. Cryst. Liq. Cryst.* **1993**, *232*, 103. (c) Shiomi, D.; Tamura, M.; Sawa, H.; Kato, R.; Kinoshita, M. *J. Phys. Soc. Jpn.* **1993**, *62*, 289.

(18) Rajca, A. *Chem. Rev.* **1994**, *94*, 871.

(19) Caneschi, A.; Gatteschi, D.; Rey, P.; Sessoli, R. *Inorg. Chem.* **1988**, *27*, 1756.

The corresponding bis(iminyl nitroxide)s behave in a similar fashion ($2J/k_B$ = + 32 K for **2,4IT** and −60 (−52 by EPR) K for **2,5IT**). These J values due to the coupling through the thiophene ring have the same sign and larger magnitude than those through the *m*-phenylene and *p*-phenylene benzene units, respectively. However, the magnetic interaction between the two radicals **N** or **I** through the bithienyl system is very much weakened to produce nearly degenerate singlet and triplet states, although the signs were barely judged to be positive for **4,5′IB** and negative for **3,3′NB** and **5,5′IB**. The complex **Mn(hfac)$_2$·2,-4NT** showed a transition to a magnet at 11 K.

The observed weak interaction in bithienyl derivatives suggests that even the polythiophene chain mentioned in the Introduction may not be an effective coupler for aligning the spins attached as pendants. However, this weak interaction must arise from small spin delocalization of nitronyl nitroxide and iminyl nitroxide radicals into the thiophene ring. Actually, the magnitude of J/k_B for nitronyl nitroxide is smaller than one-tenth of that for *tert*-butyl nitroxide radical: cf. J/k_B > 300 and = 23 K for *m*-phenylenebis(*tert*-butyl nitroxide) and **1,3NP**, respectively. If the problem of stabilities of spin sources can be overcome, thiophene, bithienyl, and poly(thiophene) chromophores should be better couplers than the corresponding phenyl rings. In preliminary experiments, *tert*-butyl nitroxide was employed as the spin source but they were unstable even at 0 °C.

Experimental Section

(A) EPR Spectroscopy and Magnetic Measurements. EPR spectra were recorded on a Bruker ESP 300 X-band (9.4 GHz) spectrometer equipped with a Hewlett-Packard 5350B microwave frequency counter. An Air Products LTD-3-110 liquid helium transfer system was attached for the low-temperature measurements. Sample solutions were placed in 4 mm o.d. quartz tubes, degassed by three freeze-and-thaw cycles, and sealed.

The magnetic susceptibility of the microcrystalline samples were measured by a Quantum Design MPMS2 SQUID system. Accurately measured ca. 30 mg of sample and 0.1 or 1 T of magnetic field were employed for the SQUID measurement. The Faraday method on an Oxford Instruments magnetic susceptibility system with a 7-T superconducting solenoid as described previously[11] was also used in the magnetization measurement for the sample in frozen matrix. One hundred microliters of 2.7 or 7.2 mM toluene solution of the sample was placed in a quartz basket with the aid of a microsyringe and used for the magnetization measurement on a Faraday magnetic balance. Data were corrected for the magnetization of 100 μL of the toluene solution without the nitroxide radical and for diamagnetic contributions which were estimated from Pascal's constants.

(B) X-ray Crystallographic Analysis. All X-ray data were collected on a Rigaku AFC-5R four-circle diffractometer using graphite-monochromated Mo Kα radiation (2.64 cm^{-1}) at 24 °C. The structures were solved in $P2_1/n$ for **2,5NT** and **4,4′NB** by direct method and converged with full-matrix least-squares using the TEXAN, Version 2.0 program (Molecular Structure Corporation). All non-hydrogen atoms were refined anisotropically; hydrogen atoms were included at standard positions (C−H 0.96 Å, C−C−H 109.5, 120, or 180°) and refined isotropically using a rigid model. Pertinent crystallographic parameters and refinement data are listed in Table 1.

Similarly, a clear red block single crystal of **2,4IT** was measured on the X-ray diffractometer and the following crystal parameters were obtained: $C_{18}H_{62}N_4O_2S$; M = 362.49; monoclinic; space group $P21/n$; a = 11.127(4) Å; b = 11.471(4) Å; c = 16.177(4) Å; β = 101.80(2)°, V = 2021.(1) Å^3; Z = 4. Further analysis of the crystal structure was hampered by disorder present in the crystal.

(C) Other Instrumentations. ^{1}H (270 MHz) and ^{13}C (68.0 MHz) NMR spectra were obtained on a JEOL GX-270 spectrometer. IR, UV−vis, and mass spectra were obtained on Hitachi I-5040 FT-IR, Hitachi U 3300, and JEOL JMS-SX 102 spectrometers, respectively. Elemental analyses were performed at the Analytical Center of this department.

(D) Materials. Solvents diethyl ether, tetrahydrofuran, 2-methyltetrahydrofuran, benzene, and toluene used for the reactions and spectral measurements were all distilled under high-purity N_2 after drying with sodium/benzophenone ketyl. Dichloromethane was distilled under high-purity N_2 after drying with calcium hydride. All reactions were stirred under an atmosphere of N_2. Anhydrous magnesium sulfate was used as the drying agent. Solvents were removed on a rotary evaporator unless otherwise stated. 2,4- and 2,5-dibromothiophene were commercially available and used as accepted.

2,4-Diformylthiophene (2,4FT). To a solution of 0.97 g of 2,4-dibromothiophene (4.01 mmol) in 200 mL of ether was added dropwise 16.8 mL of a solution of *tert*-butyllithium in *n*-hexane (1.7 M) at −78 °C. The mixture was stirred for 5 min, and then 3 mL of *N,N*-dimethylformamide was added. After stirring for 1 h, a dry ice/acetone bath was removed and the reaction mixture was allowed to warm gradually to room temperature. A yellow oil obtained by usual workup was purified by silica gel column chromatography (*n*-hexane:CH_2Cl_2 = 9:1) to afford 0.35 g of a white solid of **2,4FT** (63% yield): mp 79 −80 °C; IR (KBr) 1688, 1658 cm^{-1}; ^{1}H NMR (270 MHz, $CDCl_3$) δ 9.98 (d, 1H, J = 1.5 Hz), 9.95 (s, 1H), 8.45 (dd, 1H, J = 1.1 and 1.5 Hz), 8.17 (d, 1H, J = 1.1 Hz). Anal. Calcd for $C_6H_4O_2S$: C, 51.42; H, 2.88; S, 22.88. Found: C, 51.66; H, 3.17; S, 22.94.

2,5-Diformylthiophene (2,5FT). This was prepared by using 2,5-dibromothiophene[11g] and *n*-butyllithium in place of 2,4-dibromothiophene and *tert*-butyllithium in a manner similar to the synthesis of **2,4FT**. Purification was made by chromatography on silica gel with *n*-hexane/CH_2Cl_2 (9:1) to afford a white solid of **2,5FT** in 70% yield: mp 118−119 °C; IR (KBr) 1655 cm^{-1}; ^{1}H NMR (270 MHz, $CDCl_3$) δ 10.4 (s, 2H), 7.84 (s, 2H). Anal. Calcd for $C_6H_4O_2S$: C, 51.42; H, 2.88; S, 22.88. Found: C, 51.70; H, 2.97; S, 22.56.

2,4-Bis(1-oxy-3-oxo-4,4,5,5-tetramethyl-2-imidazolinyl)thiophene (2,4NT) and 2,4-Bis(3- oxy-4,4,5,5-tetramethyl-2-imidazolinyl)thiophene (2,4IT). A solution of 0.40 g of **2,4FT** (2.8 mmol) and 0.82 g of 2,3-bis(hydroxyamino)-2,3-dimethylbutane (5.6 mmol) in 100 mL of benzene was refluxed for 20 h while water was removed azeotropically. After removal of benzene under reduced pressure, the residue was dissolved in 200 mL of CH_2Cl_2 and 2.00 g of lead oxide was added. The suspension was stirred for 30 min, and then 1.00 g of anhydrous sodium sulfate was added. The filtrate was concentrated to dryness to give a crude mixture of **2,4NT** and **2,4IT** which was separated by chromatography on silica gel. The orange-colored first fraction with CH_2Cl_2/*n*-hexane (4:1) elution and the second dark blue fraction with CH_2Cl_2 elution gave 0.25 g of **2,4IT** (25% yield) and 0.33 g of **2,4NT** (30% yield), respectively, which were purified individually by recrystallization from *n*-hexane.

2,4NT: black blocks; mp 210−211 °C dec; UV−vis (ϵ, CH_2Cl_2) 271 (31 400), 330 (13 500), 361 (15 500), 615 (1080); EPR (9.3926 GHz, toluene) g = 2.0065 and a_N = 7.7 G, 2 N. Anal. Calcd for $C_{18}H_{26}O_4N_4S$: C, 54.80; H, 6.64; N, 14.20; S, 8.13. Found: C, 54.67; H, 6.58; N, 14.15; S, 8.43.

2,4IT: orange needles, mp 119−121 °C dec; UV−vis (ϵ, CH_2Cl_2) 261 (15 600), 469 (1100); EPR (9.3981 GHz, toluene) g = 2.0059, broad signal (ΔH_{pp} = 10.8 G). Anal. Calcd for $C_{18}H_{26}O_2N_4S$: C, 59.64; H, 7.23; N, 15.46; S, 8.85. Found: C, 59.36; H, 7.25; N, 15.27; S, 9.06.

2,5-Bis(1-oxy-3-oxo-4,4,5,5-tetramethyl-2-imidazolinyl)thiophene (2,5NT) and 2,5-Bis(3-oxy-4,4,5,5-tetramethyl-2-imidazolinyl)thiophene (2,5IT). These were prepared by using **2,5FT** in place of **2,4FT** in a manner similar to the synthesis of **2,4NT** and **2,4IT**.

2,5NT: 40% yield; black solid; mp 207−208 °C dec; UV−vis (ϵ, CH_2Cl_2) 271 (10 500), 293 (17 600), 346 (32 500), 363 (37 000), 411 (10 800), 578 (535), 623 (813), 672 (720), 805 (202); EPR (9.3917 GHz, toluene) g = 2.0065 and a_N = 7.7 G, 2 N. Anal. Calcd for $C_{18}H_{26}O_4N_4S$: C, 54.80; H, 6.64; N, 14.20; S, 8.13. Found: C, 54.56; H, 6.75; N, 14.18; S, 8.00.

2,5IT: 40% yield; brown solid; mp 175−176 °C dec; UV−vis (ϵ, CH_2Cl_2) 291 (25 500), 393 sh (1180), 503 (1130), 530 (1120); EPR (9.3987 GHz, toluene) g = 2.0060; HRMS *m/z* (relative intensity) found 362.1788 (9.1), calcd for $C_{18}H_{26}O_2N_4S$ 362.1776.

3,3′-Diformyl-2,2′-bithienyl (3,3′FB), 4,4′-Diformyl-2,2′-bithienyl (4,4′FB), and 5,5′-Diformyl-2,2′-bithienyl (5,5′FB). These were prepared by using the corresponding dibromo-2,2′-bithienyl derivatives[11]

in place of 2,4-dibromothiophene in a manner similar to the synthesis of **2,4FT**. Purification was made by chromatography on silica gel with *n*-hexane/CH_2Cl_2 (9:1) to afford white solids.

3,3′FB: 40% yield; mp 153−154 °C; IR (KBr) 1661 cm^{-1}; ^1H NMR (270 MHz, $CDCl_3$) δ 9.86 (s, 2H), 7.63 (d, 2H, J = 5.5 Hz), 7.48 (d, 2H, J = 5.5 Hz); HRMS *m/z* (relative intensity) found 221.9813 (64.4), calcd for $C_{10}H_6O_2S_2$ 221.9809.

4,4′FB: 30% yield; mp 208−209 °C; IR (KBr) 1668 cm^{-1}; ^1H NMR (270 MHz, $CDCl_3$) δ 9.88 (s, 2H), 8.06 (d, 2H, J = 1.1 Hz), 7.63 (d, 2H, J = 1.5 Hz); HRMS *m/z* (relative intensity) found 221.9833 (100), calcd for $C_{10}H_6O_2S_2$ 221.9809.

5,5′FB: 40% yield; mp 185−195 °C; IR (KBr) 1660 cm^{-1}; ^1H NMR (270 MHz, $CDCl_3$) δ 9.91 (s, 2H), 7.72 (d, 2H, J = 4.0 Hz), 7.63 (d, 2H, J = 4.0 Hz); HRMS *m/z* (relative intensity) found 221.9819 (100), calcd for $C_{10}H_6O_2S_2$ 221.9809.

4-Bromo-2,2′-bithienyl. To a solution of 1.97 g of 4,4′-dibromo-2,2′-bithienyl (6.08 mmol) in 200 mL of ether was added dropwise 7.6 mL of *n*-hexane solution of *n*-butyllithium (1.6 M) at −78 °C in 30 min. The mixture was then allowed to warm to room temperature by removal of a dry ice/acetone bath. Usual workup gave yellow solids which were chromatographed on silica gel with *n*-hexane/CH_2Cl_2 to give 0.99 g of a colorless oil (65% yield): ^1H NMR (270 MHz, $CDCl_3$) δ 7.23 (dd, 1H, J = 5.1 and 1.1 Hz), 7.15 (dd, 1H, J = 3.7 and 1.1 Hz), 7.08 (d, 1H, J = 1.1 Hz), 7.06 (d, 1H, J = 1.1 Hz), 7.00 (dd, 1H, J = 5.1 and 3.7 Hz); HRMS *m/z* (relative intensity) found 245.9012 (100), calcd for $C_8H_5BrS_2$ 245.8996.

4,5′-Diformyl-2,2′-bithienyl (4,5′FB). 4-Bromo-2,2′-bithienyl was dilithiated in a manner similar to the synthesis of **2,4FT**. The obtained yellow solid was chromatographed on silica gel with *n*-hexane/CH_2Cl_2 (9:1) elution to give white solids in 30% yield: mp 176−177 °C; IR (KBr) 1673, 1655 cm^{-1}; ^1H NMR (270 MHz, $CDCl_3$) δ 9.90 (s, 1H), 9.89 (s, 1H), 8.11 (d, 1H, J = 1.5 Hz), 7.75 (d, 1H, J = 1.5 Hz), 7.70 (d, 1H, J = 4.0 Hz), 7.33 (d, 1H, J = 4.0 Hz); HRMS *m/z* (relative intensity) found 221.9815 (100), calcd for $C_{10}H_6O_2S_2$ 221.9809.

3,3′-Bis(1-oxy-3-oxo-4,4,5,5-tetramethyl-2-imidazolinyl)-2,2′-bithienyl (3,3′NB), 4,4′-Bis(1-oxy-3 -oxo-4,4,5,5-tetramethyl-2-imidazolinyl)-2,2′-bithienyl (4,4′NB), 4,5′-Bis(3-oxy-4,4,5,5-tetramethyl-2-imidazolinyl)-2,2′-bithienyl (4,5′IB), and 5,5′-Bis(3-oxy-4,4,5,5-tetramethyl-2-imidazolinyl)-2,2′-bithienyl (5,5′IB). These were prepared by using the corresponding diformyl-2,2′-bithienyls in place of **2,4FT** in a manner similar to the synthesis of **2,4NT** and **2,4IT**. **3,3′NB** and **4,4′NB** were the major components in their reaction mixture. No nitronyl nitroxide was found in the reaction mixture for **4,5′IB** and **5,5′IB**. Separation and purification were made by chromatography on silica gel with *n*-hexane/CH_2Cl_2 elution. Recrystallization from *n*-hexane gave black crystals for all the diradicals.

3,3′NB: 35% yield; mp 158−159 °C dec; UV−vis (ϵ, CH_2Cl_2) 267 (15 600), 319 (19 500), 576 (984); EPR (9.3949 GHz, toluene) g = 2.0067 and a broad signal. Anal. Calcd for $C_{22}H_{28}O_4N_4S_2$: C, 55.44; H, 5.92; N, 11.76; S, 13.46. Found: C, 55.28; H, 5.87; N, 11.97; S, 13.57.

4,4′NB: 30% yield; mp 226−228 °C dec; UV−vis (ϵ, CH_2Cl_2) 272 (54 900), 323 (21 900), 365 (21 600), 578 (992), 623 (1540), 682 (1120); EPR (9.3950 GHz, toluene) g = 2.0067, a_N = 7.8 G, 2 N; HRMS *m/z* (relative intensity) found: 476.1564 (100), calcd for $C_{22}H_{28}O_4N_4S_2$ 476.1552.

4,5′IB: 35% yield; mp 145−151 °C dec; UV−vis (ϵ, CH_2Cl_2) 337 (19 000), 472 (920), 677 (213); EPR (9.3948 GHz, toluene) g = 2.0062, a_N = 13.2 G, $a_{N'}$ = 6.6 G; HRMS *m/z* (relative intensity) found 444.1644 (4), calcd for $C_{22}H_{28}O_2N_4S_2$ 444.1654.

5,5′IB: 20% yield; mp 157−159 °C dec; UV−vis (ϵ, CH_2Cl_2) 269 (13 200), 356 (27 900); EPR (9.3935 GHz, toluene) g = 2.0059, a_N = 13.2 G, $a_{N'}$ = 6,6 G; HRMS *m/z* (relative intensity) found 444.1635 (4), calcd for $C_{22}H_{28}O_2N_4S_2$ 444.1654.

(Hexafluoroacetylacetonato)manganese(II) 2,4-Bis(1-oxy-3-oxo-4,4,5,5-tetramethyl-2-imidazolinyl)thiophene Complex [Mn(hfac)$_2$·2,-4NT] and (hexafluoroacetylacetonato)manganese(II) 2,5-Bis(1-oxy-3-oxo-4,4,5,5-tetramethyl-2-imidazolinyl)thiophene Complex [Mn-(hfac)$_2$·2,5NT]. A solution of 94 mg of manganese(II) hexafluoroacetylacetonate dihydrate (0.185 mmol) in 100 mL of *n*-heptane was refluxed for 30 min. A solution of 36.5 mg of **2,4NT** (or **2,5NT**) in 1 mL of CH_2Cl_2 was then added with stirring at 60 °C. The solution was left in a refrigerator overnight, and the resulting precipitates were filtered off. The filtrate was concentrated to a half volume under reduced pressure and allowed to stand in a refrigerator for a week. Dark green powders (40 mg) from Mn(hfac)$_2$ and **2,4NT** gave 3Mn-(hfac)$_2$·2(**2,4NT**)·CH_2Cl_2. Anal. Calcd for $C_{66}H_{64}O_{20}N_8F_{36}S_2Mn_3$·$CH_2Cl_2$: C, 35.19; H, 2.91; N, 4.90. Found: C, 34.81; H, 2.79; N, 4.83. Dark green microcrystals from Mn(hfac)$_2$ and **2,5NT** gave Mn(hfac)$_2$·**2,-5NT**. Anal. Calcd for $C_{28}H_{28}O_2N_4F_{12}SMn$: C, 38.95; H, 3.27; N, 6.49. Found: C, 39.03; H, 3.26; N, 6.79.

Acknowledgment. This work was supported by the Grant-in-Aid for Specially Promoted Research (No. 03102003) from the Ministry of Education, Science and Culture.

Supplementary Material Available: Tables of crystallographic data and processing descriptions, final atomic coordinates, bond lengths and angles, and anisotropic thermal parameters, PLUTO drawings, a figure showing the hysteresis loop for (**2,4NT**)$_2$[Mn(hfac)$_2$]$_3$·CH_2Cl_2 at 1.8 K, and equations giving temperature dependence of χ_I, χ_S, and χ_i in eq 5 for **2,-4IT** (52 pages); tables of observed and calculated structure factors for **2,5NT** and **4,4′NB** (20 pages). This material is contained in many libraries on microfiche, immediately follows this article in the microfilm version of the journal, can be ordered from the ACS, and can be downloaded from the Internet; see any current masthead page for ordering information and Internet access instructions.

JA943072X